Brain Hemorrhages 3 (2022) 57–61

Contents lists available at ScienceDirect

Brain Hemorrhages

journal homepage: www.keaipublishing.com/en/journals/brain-hemorrhages/

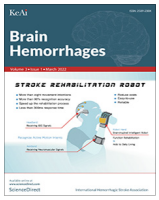

Research article

Colorimetry for wall appearance study of cerebral aneurysms

Takenori Sato [a,b,*], Fujimaro Ishida [c], Satoru Tanioka [c], Yoichi Miura [b], Katsuhiro Tanaka [c], Hidenori Suzuki [b]

[a] Department of Internal Medicine, Kinan Hospital, Minamimuro-gun, Mie, Japan
[b] Department of Neurosurgery, Mie University Graduate School of Medicine, Tsu, Mie, Japan
[c] Department of Neurosurgery, Mie Chuo Medical Center, National Hospital Organization, Tsu, Mie, Japan

ARTICLE INFO

Article history:
Received 21 September 2021
Received in revised form 23 October 2021
Accepted 26 October 2021
Available online 30 October 2021

Keywords:
Cerebral aneurysm
Aneurysm wall characteristics
Colorimetry
CIE $L^*a^*b^*$
Digital Color Meter
Aneurysm Red Indicator

ABSTRACT

Background: Neurosurgeons can assess thin red walls in a cerebral aneurysm during a microsurgical procedure, but the judgment of the color is subjective and could have a bias. This study aimed to quantitatively evaluate the aneurysm wall characteristics.
Methods: In 15 unruptured cerebral aneurysms, the surface color of cerebral aneurysms, parent arteries and branches were measured using Commission International del'Eclairage $L^*a^*b^*$. The values of L^* (perceptual lightness), a^* (red-green color characteristics) and b^* (blue-yellow color characteristics) were compared with color discrimination by two independent neurosurgeons, which was classified into "red", "yellow", "white" and "unjudged".
Results: Significantly lower L^* and higher a^* values were shown in red wall points consistently judged by both neurosurgeons compared with yellow or white wall points, while b^* values had no significant differences. Based on these results, a novel index, aneurysm red indicator (ARI) was developed as a ratio of a^* to L^* values. The ARI had a high sensitivity and specificity to discriminate red walls (0.984 and 0.986, respectively).
Conclusions: ARI could be useful for evaluating thin red walls of cerebral aneurysms. The novel approach using colorimetry may contribute to future hemodynamics analyses related to the aneurysm wall characteristics.

1. Introduction

Unruptured cerebral aneurysms have the potential to cause subarachnoid hemorrhage, which often results in death. Therefore, preventive surgery such as neck clipping or endovascular coiling is performed to avoid the rupture of cerebral aneurysms. It is crucial to evaluate aneurysm location, size and structural relationships for optimal surgical strategy. Neuroimages such as computed tomography (CT) and cerebral angiography (CAG) are adopted to collect the anatomical information. Recent advance in neuroimaging has made it possible to depict the accurate 3D images of cerebral aneurysms; however, the vasculature in these images corresponds to the blood flow domain with a contrast medium. Therefore, it is impossible to show or predict the aneurysm wall characteristics.

Neurosurgeons can observe several types of aneurysm walls including a thin red wall or atherosclerotic changes during a microsurgical procedure. These findings are pathologically caused by degeneration of vascular intima, and perceived as replacement to fibrin and inflammatory cells, thinning or hypertrophy of a wall. Since the degeneration is related to hemodynamics, several computational fluid dynamics (CFD) studies using preoperative images have demonstrated that hemodynamic parameters can predict a thin red wall and an atherosclerotic change in an aneurysm wall.[1–4] Thin red walls suggest destructive remodeling, and an atherosclerotic change is observed as a yellowish wall or hyperplastic remodeling.[5–7] Since the judgment of an aneurysm wall has been made based on the aneurysm wall color in the microsurgical movie, the results could have a bias by each observer.

Commission International del'Eclairage (CIE) $L^*a^*b^*$ is one of colorimetric approaches of which colors are expressed in 3-dimensional color space. L^* value indicates perceptual lightness, a^* value indicates red-green color characteristics and b^* value indicates blue-yellow color characteristics. This approach is based on the way how humans perceive colors. Accordingly, illumination, size of samples or background color can affect the values. In this study, we adopted colorimetry using CIE $L^*a^*b^*$ to make quantitative evaluation of the aneurysm wall characteristics, and developed a new colorimetric index.

* Corresponding author at: Department of Neurosurgery, Mie University Graduate School of Medicine, 2-174 Edobashi, Tsu, Mie 514-0001, Japan.
E-mail address: m11048ts@jichi.ac.jp (T. Sato).

https://doi.org/10.1016/j.hest.2021.10.002

2. Materials and methods

2.1. Patient population and image data acquisition

This study was conducted in accordance with the guideline and under the approval of the ethics review board of Mie Chuo Medical Center. We reviewed our database of patients with unruptured cerebral aneurysms treated at Mie Chuo Medical Center between 2016 and 2017. The inclusion criteria were unruptured cerebral aneurysms that were exposed sufficiently under the microsurgical observation. Consequently, 15 unruptured cerebral aneurysms in 14 patients were included in this study. There were 7 middle cerebral artery, 6 internal carotid artery, 1 anterior cerebral artery, and 1 anterior communicating artery aneurysms (Table 1). The microsurgical procedures were recorded by OPMI Pentero800 (Carl Zeiss Microscopy) with MKC-300HD (Ikegami, 1080p, 60 Hz) and VC-50HD (Roland). Intraoperative images were captured just before the neck clipping.

2.2. Design of the analysis

The Digital Color Meter (DCM) that is a utility of Macintosh computer was employed to measure the color values (L^*, a^* and b^*) of pixels on the intraoperative images of an aneurysm surface wall. All images were attached on the center of keynote slides on MacBook® (Retina, 12-inch, 2017, macOS Mojave) by square with sides 768pt, and 130 perfect circles were located on slides adjacently (Fig. 1). Diameter of the circles was 76pt. Small squares with sides 14pt were located in the center of the circles (Fig. 1). We numbered the small squares on cerebral aneurysms, parent arteries and branches and measured each value of L^*, a^* and b^*. Aperture size of DCM was the largest one (Fig. 2). In advance, the points of reflected light of the operating microscope that were defined by $L^* \geq 93$, $-5 \leq a^* \leq 5$, and $-5 \leq b^* \leq 5$ were excluded. Macroscopic color findings of the small squares were classified into "red", "yellow", "white", and "unjudged", which were judged by two independent neurosurgeons. We compared the values of L^*, a^* and b^* with the macroscopic color findings.

2.3. Statistical analysis

Statistical analysis was made using EZR software (Saitama Medical Center, Jichi Medical University, Saitama, Japan, version 1.41) for Mann-Whitney U tests, Kruskal Wallis tests and receiver-operating characteristics (ROC) curve analyses. A statistical significance was considered if a P-value was<0.05.

3. Results

3.1. The number of square points and macroscopic color findings

Seventy-seven points from cerebral aneurysms, 124 points from parental arteries and 177 points from branches (total 378 points) were extracted on the intraoperative images (Table 1). Four points were excluded because they corresponded to the conditions of reflected light. In independent judgments by two neurosurgeons, the number of points that both of them judged red (red-red; RR), yellow (yellow-yellow; YY), white (white-white; WW), and unjudged (unjudged-unjudged; UU) was 62, 34, 36, and 105, respectively. We defined YY and WW points as non-red (nonR) points, of which the number was 70. The judgments of other 141 points were discrepant between the 2 neurosurgeons: among them, 97 points were judged red by either neurosurgeon (red-unjudged in 96 points; and red-yellow in 1 point) which were defined as red-others (R) points.

3.2. Comparison of values of L^*, a^* and b^*

Comparison of L^*, a^* and b^* values was administered between RR and nonR points. On statistical evaluation, L^* values were significantly lower but a^* values were significantly higher in RR points than in nonR ones, and b^* values had no significant differences between RR and nonR points (42.2 versus 82.0, $P < 0.001$; 46.7 versus 12.7, $P < 0.001$; and 19.0 versus 15.0, $P = 0.714$, respectively; Table 2).

3.3. Aneurysm red indicator (ARI)

Since RR points had high a^* and low L^* values, we developed a novel index, ARI, which was the ratio of a^* to L^* values. The ARI was significantly higher in RR points than in nonR ones (1.2 versus 0.15, $P < 0.001$; Table 2). On a ROC curve analysis for the performance of ARI according to the discrimination between RR and nonR points, the sensitivity was 98.4%, and the specificity was 98.6% (area under the curve, 0.999; 95% confidence interval, 0.997–1; cut off value, 0.695; Fig. 3). Furthermore, when ARI was compared among RR, R and nonR points, there was a significant difference (median value, 1.201, 0.698, and 0.148, respectively; $P < 0.001$). In a Steel-Dwass analysis, ARI in RR points was significantly higher than that

Table 1
Location of cerebral aneurysms and judgment of the color.

Case No.	Aneurysm location	RR point	R point	nonR point
1	MCA	4	9	8
2	ICA	9	11	11
3	ICA	0	7	2
4	MCA	10	3	11
5	MCA	5	0	4
6	ACA	11	5	1
7	ICA	0	10	5
8	MCA	2	17	1
9	ICA	2	5	4
10	ICA	0	1	5
11	MCA	7	9	1
12	MCA	1	4	0
13	ACOM	8	7	1
14	ICA	1	2	10
15	MCA	2	7	6

Values indicate the number of each point. ACA, anterior cerebral artery; ACOM, anterior communicating artery; ICA, internal carotid artery; MCA, middle cerebral artery; nonR, non-red wall consistently judged by both of two independent neurosurgeons; R, red wall judged by one of two independent neurosurgeons; RR, red wall consistently judged by both of two independent neurosurgeons.

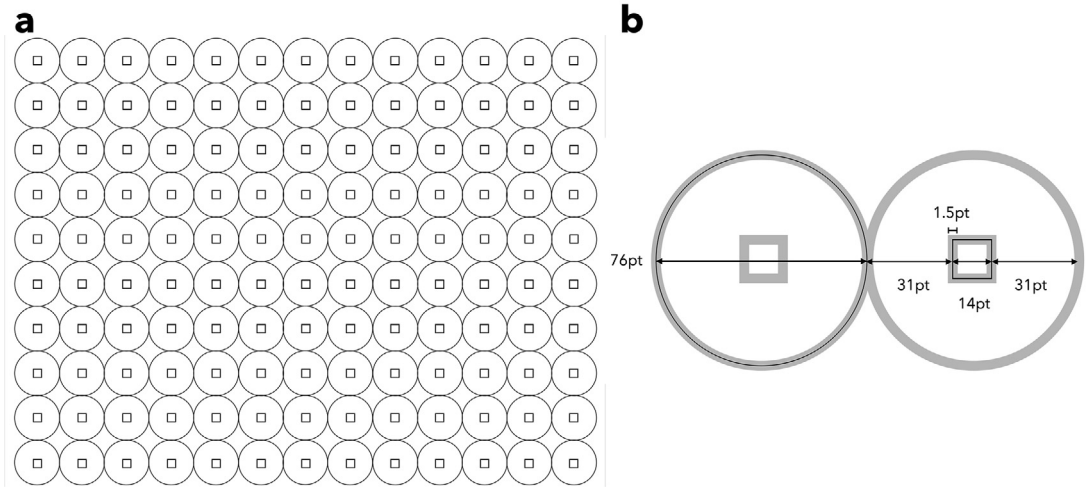

Fig. 1. Disposition (**a**) and regulation (**b**) of perfect circles and squares.

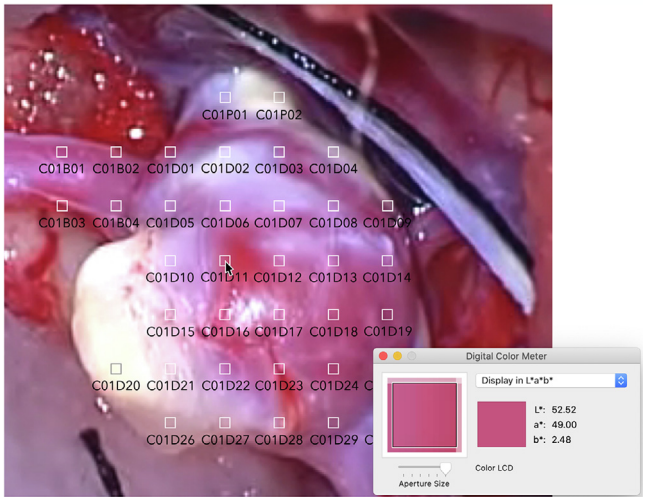

Fig. 2. Intraoperative image of middle cerebral artery aneurysm with atherosclerotic change. L^*, a^*, b^* values at the squares are measured using Digital Color Meter (DCM). The frame of DCM is located in the center of the squares. B indicates branch; C, case; D, dome; and P, parent artery.

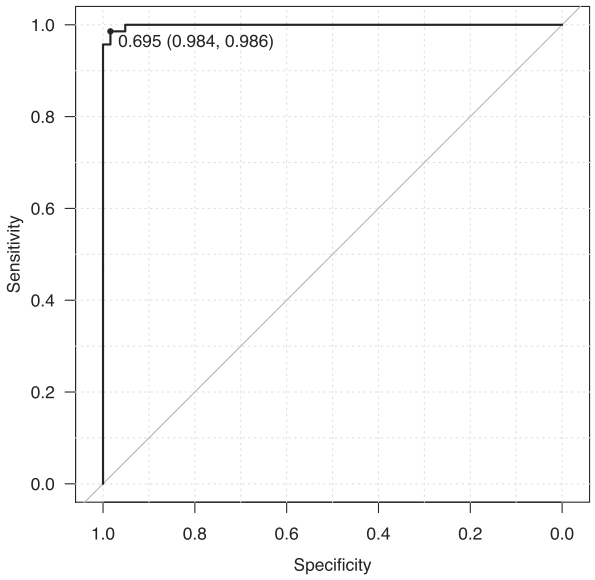

Fig. 3. Receiver-operating characteristics curve analysis for the performance of aneurysm red indicator according to the discrimination between red and non-red walls consistently judged by two independent neurosurgeons. Values indicate a cut off value (sensitivity, specificity).

Table 2
Values of L^*, a^*, b^* and a^*/L^* at red-red (RR) and non-red (nonR) points of cerebral aneurysm walls.

Color expression or index	RR point (n = 62)	nonR point (n = 70)	P value*
L^*	42.2 (18.6–58.1)	82.0 (38.2–99.6)	0.001
a^*	46.3 (22.0–71.6)	12.7 (−6.92–30.4)	0.001
b^*	19.0 (-9.36–47.0)	15.0 (−22.1–58.4)	0.714
a^*/L^*	1.20 (0.56–1.84)	0.15 (−0.07–0.79)	0.001

Values are the median (interquartile range). nonR, non-red wall consistently judged by both of two independent neurosurgeons; RR, red wall consistently judged by both of two independent neurosurgeons. *Mann-Whitney *U* test.

in both R and nonR points, and ARI in R points was significantly higher than that in nonR points (Fig. 4).

4. Discussion

Predicting thin red wall regions of cerebral aneurysms play an important role in making decision for precise surgical strategy. Recent studies revealed that subjective reddish areas of cerebral aneurysm walls in an intraoperative view suggested destructive changes in the vascular intima, and that aberrant hemodynamics caused an aneurysm wall to be increasingly weaker and prone to rupture.[8] However, studies as to quantitative analyses of the color of cerebral aneurysm walls are limited. Cho et al. analyzed the characteristics of cerebral aneurysm walls using CIE $L^*a^*b^*$ and hemodynamic parameters, and concluded that reddish areas of cerebral aneurysm walls were hemodynamically in danger of rupturing.[9] They focused on a difference between two colors, and tried to prescribe objective reddish areas in cerebral aneurysm walls by comparing subjective reddish areas with the other areas. However, the reddish wall was not defined clearly in the study.[9] Therefore, we focused on colors based on the remodeling of cerebral aneurysm walls, and compared reddish points with yellowish and whitish points using CIE $L^*a^*b^*$ with the sufficient sample size. The a^*

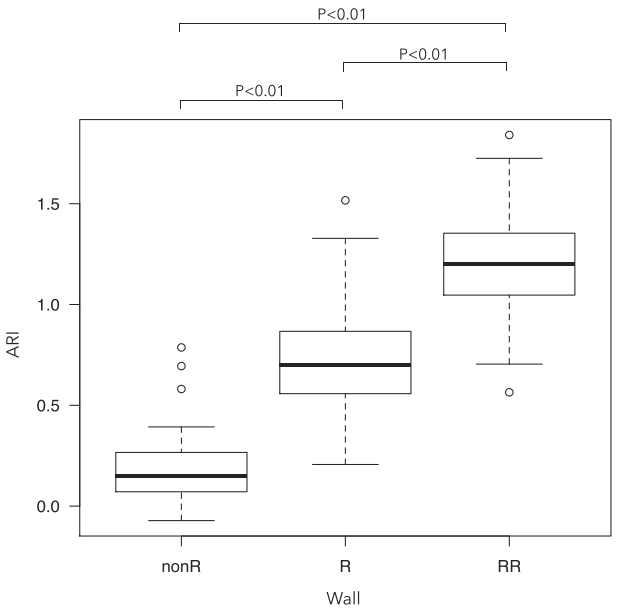

Fig. 4. Aneurysm red indicator (ARI) in non-red (nonR), red (R) and red-red (RR) aneurysmal wall points. nonR, non-red consistently judged by both of two independent neurosurgeons; R, red judged by one of two independent neurosurgeons; RR, red consistently judged by both of two independent neurosurgeons. Data indicate median ± 25–75 percentiles. P values are determined by Steel-Dwass analyses.

value was significantly higher as expected, but the L^* value was unexpectedly lower in reddish points of cerebral aneurysmal walls. It means that neurosurgeons' recognition of thin red walls is affected by not only a^* values but L^* values, and therefore we developed ARI that is the ratio of a^* to L^* values. Because ARI had a very high sensitivity and specificity, thin red walls of cerebral aneurysms can be evaluated by ARI.

Since darkness environment can lead to a bias, the sufficient number of dissected aneurysms during microsurgery is desirable to analyze and determine the color characteristics of the aneurysm walls. In addition, reflected light can be confused with a whitish wall, and therefore reflected light should be ruled out based on the conditions of reflected light. White balance calibration and illumination adjustment of microscope should be also performed for accurate color analysis. In our study, there were few dark points on measurement points, and most of unjudged points were due to the difficulty in judging the color as red, yellow or white. But there were some points which had mixed colors because of the size of a square like C01D23 in Fig. 2. However, the phenomena might be inevitable in the recognition of the color.

CIE $L^*a^*b^*$ was established in 1976 based on the opponent theory of the color vision that can be grouped into three opponent pairs, white/black, red/green and yellow/blue.[10] CIE $L^*a^*b^*$ has been a public domain and freely used, because it is defined mathematically and license free. For example, CIE $L^*a^*b^*$ model is employed in Adobe Photoshop, Affinity Photo, PDF documents, DCM on macOS and others. DCM on macOS has been used to analyze colors of various materials in some studies.[11–14] It is a free application on macOS, and can simply and usefully measure colors with $L^*a^*b^*$ and RBG systems. We can measure the values of L^*, a^* and b^* of all colors on a desktop screen easily using DCM, and it is a simple approach to evaluate aneurysm wall color on intraoperative images objectively. Recently, other methods of colorimetry have been established such as a color appearance model (CAM).[15,16] Progressive studies of cerebral aneurysm wall characteristics will be developed using further methods of colorimetry; however, a reddish wall of cerebral aneurysms could be defined by CIE $L^*a^*b^*$ on DCM. It is meaningful that the analysis with a high diagnostic value can be performed using free software.

On the basis of findings obtained by colorimetry using CIE $L^*a^*b^*$, we are able to evaluate the aneurysm wall color characteristics more accurately and objectively. This method can serve as a basis for future studies on aneurysm wall colorimetric characteristics. In addition, by the comparison with a novel index ARI, future studies would allow us to predict intraoperative aneurysm wall properties based on preoperative aneurysm geometry, flow characteristics, magnetic resonance imaging for vessel wall examination and several hemodynamic parameters. The novel approach using colorimetry will bring about more optimal validation of more and more developing CFD hemodynamics related to the aneurysm wall characteristics on the judgment by ARI.

5. Conclusions

The characteristics of cerebral aneurysm walls observed during microsurgery can be analyzed quantitatively by the colorimetric approach, which may evaluate a thin red wall like experienced neurosurgeons. Our findings will be useful in validating the findings of CFD and other methods, contributing to the realization of preoperative prediction of cerebral aneurysm wall characteristics using methods such as CFD.

Ethical approval

This study was conducted in accordance with the guideline and under the approval of the ethics review board of Mie Chuo Medical Center. Informed consent was waived because of the retrospective nature of this study, which was approved by the ethics review board of Mie Chuo Medical Center.

Funding

The authors received no specific funding for this work.

Declaration of Competing Interest

The authors declare that they have no known competing financial interests or personal relationships that could have appeared to influence the work reported in this paper.

Consent for publication

All the authors have consented for publication of this manuscript.

References

1. Sforza DM, Putman CM, Cebral JR. Hemodynamics of cerebral aneurysms. *Annu Rev Fluid Mech.*. 2009;41(1):91–107.
2. Metaxa E, Tremmel M, Natarajan SK, et al. Characterization of critical hemodynamics contributing to aneurysmal remodeling at the basilar terminus in a rabbit model. *Stroke*. 2010;41(8):1774–1782.
3. Suzuki T, Takao H, Suzuki T, et al. Determining the presence of thin-wall regions at high-pressure areas in unruptured cerebral aneurysms by using computational fluid dynamics. *Neurosurgery.*. 2016;79:589–595.
4. Hidehito K, Masaaki T, Kosuke H, et al. Clear detection thin-walled regions in unruptured cerebral aneurysms by using computational fluid dynamics. *World Neurosurg.*. 2019;121:287–295.
5. Meng H, Wang Z, Hoi Y, et al. Complex hemodynamics at the apex of an arterial bifurcation induces vascular remodeling resembling cerebral aneurysm initiation. *Stroke*. 2007;38(6):1924–1931.
6. Nabaei M, Fatouraee N. Microstructural modelling of cerebral aneurysm evolution through effective stress mediated destructive remodeling. *J Theor Biol.*. 2014;354:60–71.

7. Furukawa K, Ishida F, Tsuji M, et al. Hemodynamics characteristics of hyperplastic remodeling lesions in cerebral aneurysms. *PLoS ONE*. 2018;13 e0191287.
8. Meng H, Tutino VM, Xiang J, Siddiqui A. High WSS or low WSS? Complex interactions of hemodynamics with intracranial aneurysm initiation, growth, and rupture: toward a unifying hypothesis. *Am J Neuroradiol.*. 2014;35 (7):1254–1262.
9. Cho K-C, Choi JH, Oh JH, Kim YB. Prediction of thin-walled areas of unruptured cerebral aneurysms through comparison of normalized hemodynamic parameters and intraoperative images. *Biomed Res Int.*. 2018;2018:1–9.
10. Gilchrist A, Nobbs J. Colorimetry, Theory. Encyclopedia of spectroscopy and spectrometry. 1999;337-343.
11. Abe K, Suzuki K, Citterio D. Inkjet-printed microfluidic multianalyte chemical sensing paper. *Anal Chem.*. 2008;80(18):6928–6934.
12. Schnell AK, Smith CL, Hanlon RT, Harcourt R. Giant Australian cuttlefish use mutual assessment to resolve male-male contests. *Animal Behavior.*. 2015;107:31–40.
13. Nakano S, Makino K, Yoshida I, et al. Combined influences of iron-oxides and micropores on reddish coloration of alkali feldspars in granitic rocks. *J Geol Soc Japan.*. 2019;125(10):759–773.
14. Polubothu S, Kinsler VA. Final congenital melanocytic nave colour is determined by normal skin colour and unaltered by superficial removal techniques: a longitudinal study. *Br J Dermatol.*. 2020;182:721–728.
15. Li C, Li Z, Wang Z, et al. Comprehensive color solutions: CAM16, CAT16, and CAM16-UCS. *Color Res Appl.*. 2017;42(6):703–718.
16. Thwaites A, Wingfield C, Wieser E, Soltan A, Marslen-Wilson WD, Nimmo-Smith I. Entrainment to the CIECAM02 and CIELAB colour appearance models in the human cortex. *Vision Res.*. 2018;145:1–10.